

<sup>27</sup> Creager, M. O., "The Effect of Leading-Edge Sweep and Surface Inclination on the Hypersonic Flow Field Over a Blunt Flat Plate," Memo 12-26-58A, Jan. 1959, NASA.

<sup>28</sup> Coleman, H. W. and Lemmon, E. C., "Turbulent Heat Transfer and Pressure on Leading Edges of Fins Mounted on a Cone," SCL-RR-720308, 1972, Sandia Lab., Livermore, Calif.

<sup>29</sup> Markarian, C. F., "Heat Transfer in Shock Wave Boundary Layer Interaction Regions," NWC TP 4485, Nov. 1968, Naval Weapons Center, China Lake, Calif.

<sup>30</sup> Beckwith, I. E. and Gallagher, J. J., "Local Heat Transfer and

Recovery Temperatures on a Yawed Cylinder at Mach Number of 4.15 and High Reynolds Numbers," TR R-104, 1958, NASA.

<sup>31</sup> Hunt, J. L., Bushnell, D. N., and Beckwith, I. E., "The Compressible Turbulent Boundary Layer on a Blunt Swept Slab With and Without Leading-Edge Blowing," TN D-6203, March 1971, NASA.

<sup>32</sup> Bertram, M. H. and Henderson, A., Jr., "Some Recent Research With Viscous Interacting Flow in Hypersonic Streams," *Proceedings of the Symposium on Viscous Interaction Phenomena in Supersonic and Hypersonic Flow*, Hypersonic Research Labs., Aerospace Research Labs., May 1969, pp. 1-30.

NOVEMBER 1973

J. SPACECRAFT

VOL. 10, NO. 11

## Static Stability and Drag Studies for Bodies of Revolution in Supersonic Flow

HANS-JOACHIM LUCKERT\*

*Space Research Corporation, Montreal, Quebec, Canada*

Reliable estimates of stability and performance characteristics are essential for the design of missiles, shells, and space probes. Particularly in the case of parametric studies to determine the optimum configuration for a specific mission, an inexpensive and simple method is needed. The second-order shock expansion theory of Syvertson and Dennis was found to meet these requirements. The method, somewhat modified for concave corners, was therefore used in practical applications for bodies of revolution in axisymmetric flow. Example calculations show the usefulness of the method for comparison of configurations, such as ogival and parabolic, or tangent and secant contours. Applied to configurations with flares considerable differences from conventional results with the Newtonian theory were obtained; the differences depend strongly on Mach number, flare length and angle. A further application deals with the effect of forebody on afterbody. Comparison with test results confirm the predictions. The method is therefore especially useful for preliminary design studies for which more sophisticated theories or experimental programs would be uneconomical regarding cost and time.

### Nomenclature

$a, b$  = constants in equation for pressure [Eq. (2)]  
 $C_1$  = characteristic coordinate  
 $C_{DW}$  = wave drag coefficient =  $\text{Drag} / [(\gamma/2) M_\infty^2 p_\infty S_{\text{ref}}]$   
 $C_N$  = normal force coefficient =  $\text{Normal Force} / [(\gamma/2) M_\infty^2 p_\infty S_{\text{ref}}]$   
 $C_{N\alpha} = \partial C_N / \partial \alpha$   
 $d, D$  = diameter  
 $f$  = fineness ratio ( $= L/D$ )  
 $K_D$  = ballistic drag force coefficient =  $(\pi/8) C_D$   
 $K_N$  = ballistic normal force coefficient =  $(\pi/8) C_{N\alpha}$   
 $l, L$  = length  
 $M$  = Mach number  
 $p$  = pressure  
 $r, R$  = radius  
 $s$  = coordinate along body contour  
 $S$  = cross section area  
 $s_g$  = gyroscopic stability factor  
 $x, x'$  = coordinate along body axis from nose ( $x$ ) or tail ( $x'$ )  
 $\alpha$  = angle of attack, rad  
 $\gamma$  = ratio of specific heats ( $= 1.4$ )  
 $\delta$  = semivertex angle, deg  
 $\mu$  = Mach angle

$\xi$  = contour coordinate,  $= x/L$   
 $\eta$  = contour coordinate,  $= d/D = r/R$

### Subscripts

1, 2, 3, 4 = positions on body  
 $c$  = cone  
 $tc$  = tangential cone of body element  
 $cp$  = center of pressure  
 $\text{ref}$  = reference  
 $B$  = base  
 $S$  = secant  
 $T$  = tangent

### Introduction

MISSILES, upper atmosphere research vehicles, and shells have the principal requirements of reaching a given altitude or range with a certain degree of aerodynamic or gyroscopic stability. In either case it is essential to predict the stability characteristics, the normal force curve slope and the center of pressure, as well as the drag as accurately as possible in order to achieve the most suitable configuration for the given requirements.

The present study deals only with bodies of revolution in symmetric flow. Various design charts and handbooks are available to estimate the required aerodynamic characteristics for simple configurations, such as cone-cylinder or ogive-cylinder combinations, conical flares, or boattails.<sup>1-3</sup> Some

Presented as Paper 73-295 at the AIAA 3rd Sounding Rocket Technology Conference, Albuquerque, N. Mex., March 7-9, 1973; submitted March 29, 1973; revision received June 27, 1973.

Index categories: LV/M Aerodynamics; Aircraft Configuration Design.

\* Chief Aerodynamicist. Associate Fellow AIAA.

of these charts or suggested calculation methods are based on experimental data in combination with theory while others result from theoretical considerations, as for example in the case of flares and boattails following a semi-infinite cylinder, and do not account for the actual forebody effect.

The practical design engineer, however, is faced with the problem of using arbitrary contours or compound configurations consisting of sections of various basic contour shapes, e.g., combinations of ogival, parabolic, conical, cylindrical, or other forms. In these cases the generally available design charts<sup>1-3</sup> can only give rough approximations which are not satisfactory for the purpose in question, and which may also give misleading results. Experimental results obtained from wind tunnel and aeroballistic range tests are not only very expensive and time consuming but also highly uneconomical for a parametric study to obtain an optimum configuration. For preliminary design studies, therefore, the best solution would be a quick, handy, inexpensive and simple method yet giving good agreement with tests.

The second-order shock expansion method of Syvertson and Dennis<sup>4</sup> appears to be the most convenient for this purpose. In a study directed by the author and supported by a grant from the Canadian National Research Council a computer program was set up. The initial aim was to investigate the effect of flares (conical frustra) depending on Mach number, flare length and angle for comparison with the usually applied Newtonian impact theory. Results of this study, including the effects of forebody on afterbody for various basic configurations, are given in a Master's thesis at McGill University.<sup>5</sup>

The present paper intends only to show some theoretical results (obtained with the second-order shock expansion method) for design applications which might be of interest to the practical engineer. Its aim is also to show that the method used, based on theoretical input data for cones, is not only convenient and inexpensive but in good agreement with experimental data and therefore fully satisfactory for preliminary design studies.

### The Second-Order Shock Expansion Method

Only a brief review of this method may be given here. It is a refinement of the generalized shock expansion method for bodies of revolution, which was based on the following assumptions and approximations.

1) Disturbances incident on an oblique shock wave are largely absorbed therein, and hence, reflected disturbances are negligible. 2) The flow is assumed to be locally two dimensional. 3) Surface streamlines are taken as meridian lines.

Combining the continuity, momentum, energy and state equations with the characteristics theory, the equation for the streamline pressure gradient on nonlifting bodies then takes the form<sup>4</sup>

$$\frac{\partial p}{\partial s} - \frac{\gamma p M^2}{(M^2 - 1)^{1/2}} \cdot \frac{\partial \delta}{\partial s} = \frac{1}{\cos \mu} \cdot \frac{\partial p}{\partial C_1} \quad (1)$$

where  $C_1$  is a characteristic coordinate.

The basic ideas of the second-order shock expansion method are to approximate the body by a large number of conical frustrum elements (with either tangents or secants<sup>6</sup> to the original contour), and to replace the right-hand side of Eq. (1) by a series in  $p$  and  $s$ . For short elements the use of the first term, a linear expression in  $p$ , is sufficient so that Eq. (1) becomes

$$\partial p / \partial s = a \cdot (b - p) \quad (2)$$

By integration the pressure along the contour of such a frustrum element, as shown in Fig. 1 is obtained if the conditions at the start of the element (point 2) are known and if conical values for an infinitely long frustrum are assumed. The

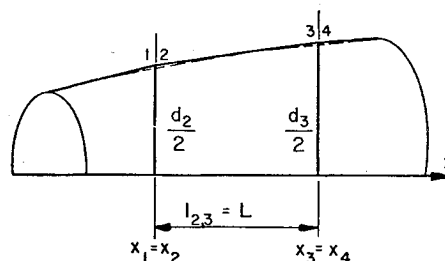


Fig. 1 Frustrum element approximating actual body element.

initial conditions of the element, however, are obtained by a Prandtl-Meyer expansion for a convex corner or an oblique shock compression for a concave corner.

With the pressure distribution known, the zero lift drag coefficient as well as the normal force curve slope and the center of pressure can be determined. Details of the method and the relevant calculation procedure can be found in the report by Syvertson and Dennis.<sup>4</sup>

The method was implemented as a digital computer program for  $n$  elements,<sup>5</sup> tangent and secant approximations of the actual contour were used and the average of the two results taken. In the case of concave corners a slightly different approach was made; the Syvertson-Dennis equations were replaced by using an extension of a method by Mölder<sup>7</sup> for two-dimensional flow to the axisymmetric case. This method gives the gradient of the flow variables across a shock wave. It was found to be in agreement with results obtained with a different approach by Geber and Bartos.<sup>8</sup>

The only input data required for the method are the angle  $\delta$ , the normal force coefficient  $C_{N_{atc}}$  and the pressure coefficient  $C_{p_{tc}}$  of the tangent cones for each element and Mach number. The cone data used are those obtained from the conical theory.

### Ogives and Paraboloids

An ogive, either tangent or secant, is often used as the forebody of a shell or missile because it appears to be the most favorable choice as to volume and performance for a given mission. The nondimensional equation for the tangent ogive with  $L$  = length,  $D$  = diameter,  $f = L/D$ ,  $\xi = x/L$  (from tip),  $\eta = d/D$  is given by

$$\eta = 1 + 2\{[(f^2 - 1/4)^2 + f^2(2\xi - \xi^2)]^{1/2} - (f^2 + 1/4)\} \quad (3)$$

For large  $f$  this equation approaches

$$\eta = 2\xi - \xi^2 \quad (4)$$

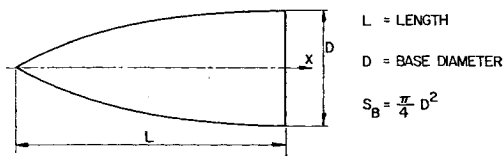
which is the equation of a tangent parabola with the vertex at  $\xi = 1$ .

A comparison of the meridian curves of tangent ogives with those of tangent parabolas shows that the difference is negligible for fineness ratios  $f \geq 3$ , and is very small even for a fineness ratio as low as 2.

In practical applications the chosen fineness ratio is usually much larger than 2, mainly for drag reasons, so that ogival and parabolic contours appear to be equivalent. To see whether there is a difference aerodynamically, the second-order shock expansion method was applied to small fineness ratios (2 and 3) where the largest difference could be expected. The results given in Table 1 indicate that the differences between the aerodynamic data are in the order of the accuracy of the calculation. The differences between the volumes are also small so that none of the contours appears superior over the other from these points of view. One advantage of the ogive is that for purposes of manufacture the contour can be described by a single radius. On the other hand, a parabolic contour, tangent or secant, has a number of advantages since all equations (Fig. 2) become simple and all form coefficients

Table 1 Comparison ogives vs paraboloids

		$C_{N\alpha}$	$X_{cp}/d$	$C_{Dw}$	$\text{Vol}/S_B L$
2-caliber ogive and paraboloid					
$M=2$	OG	2.034	1.058	0.1950	0.5428
	PAR	2.035	1.070	0.1950	0.5333
$M=3$	OG	1.936	1.042	0.1709	
	PAR	1.960	1.052	0.1723	
$M=4$	OG	1.715	1.003	0.1550	
	PAR	1.740	1.014	0.1557	
3-caliber ogive and paraboloid					
$M=3$	OG	2.212	1.579	0.0915	0.5375
	PAR	2.202	1.586	0.0909	0.5333



VOLUME  $\text{VOL.} = \frac{\pi}{15} S_B L$  C.G. of VOLUME  $X_V = \frac{11}{16} L$

WETTED AREA  $S_W = \frac{2}{3} \pi D L$  C.G. of WETTED AREA  $X_W = \frac{5}{8} L$

PROJ. AREA  $S_P = \frac{2}{3} D L$  C.G. of PROJ. AREA  $X_P = \frac{5}{8} L$

NOTE. C.G. MEASURED FROM VERTEX

Fig. 2 Tangent paraboloids.

are independent of the fineness ratio (also for the wetted area terms if the approximations  $\int \eta d\xi$  and  $\int \eta \xi d\xi$  are used). Furthermore, simple relations are obtained between the tangent and secant parabolas of the same fineness ratio and the corresponding tangent parabola of which the secant parabola is a part, as seen in Fig. 3.

Results obtained with the second-order shock expansion method for a 5 cal tangent paraboloid (or ogive) with and without a 1.5 cal cylindrical afterbody are compared in Fig. 4 with results from other methods.<sup>1-3</sup> There is either good agreement for small Mach numbers, or for larger Mach numbers. The comparison of the wave drag curve is particularly instructive: the DATCOM<sup>1</sup> results are in agreement with the theory for  $M > 2.5$ , and have a similar trend as the theory for  $M < 2.5$ , whereas the data from Refs. 2 or 3 give a better approximation for small  $M$ . The curve obtained with the second order shock expansion method appears as the best choice since it evidently does not underestimate the drag.

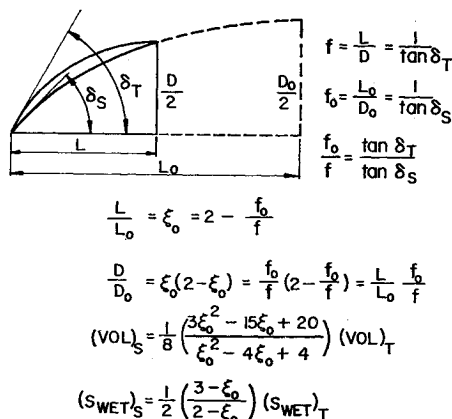


Fig. 3 Relations between tangent and secant paraboloids.

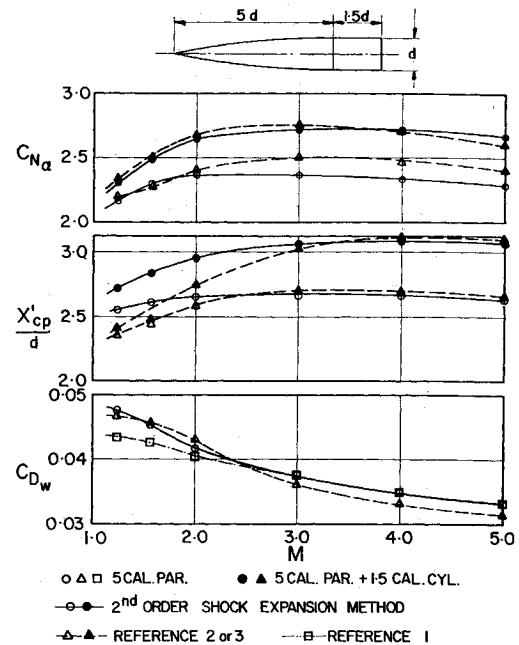


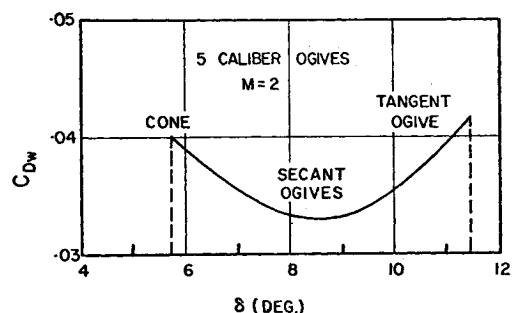
Fig. 4 Comparison of results from the second-order shock expansion method and design graphs for a 5-caliber paraboloid with and without a 1.5-caliber cylindrical afterbody.

In general, it is thought that the theoretical data are more reliable and especially more useful for preliminary design work involving a parametric study and comparisons. Available test data (as discussed in the following sections) confirm the reliability of the method.

### Secant vs Tangent Ogives

Secant ogives have frequently been used for shell and missile configurations since they have a more favorable drag than tangent ogives of the same fineness ratio. Theory confirms the empirical results: the application of the second-order shock expansion method to five-caliber ogives with varying semi-vertex angles  $\delta$  shows that the smallest wave drag is obtained about midway between the two extreme cases of a tangent ogive ( $\delta = 11.42^\circ$ ) and a cone ( $\delta = 5.71^\circ$ ), as seen in Fig. 5 for  $M=2$ . In this case the wave drag at  $\delta \approx 8.5^\circ$  is about 20% smaller than that of the cone and the tangent ogive.

The secant ogive also appears to be preferable regarding the stability characteristics. Table 2 and Fig. 6 compare the normal force derivative, the center of pressure and the wave drag data of a five-caliber tangent ( $\delta = 11.31^\circ$ ) with those of a five-caliber secant paraboloid ( $\delta = 8.5^\circ$ ), with and without a 1 caliber cylindrical afterbody, for various Mach numbers.

Fig. 5 Wave drag coefficient  $C_{Dw}$  vs semivertex angle  $\delta$  for 5-caliber ogives.

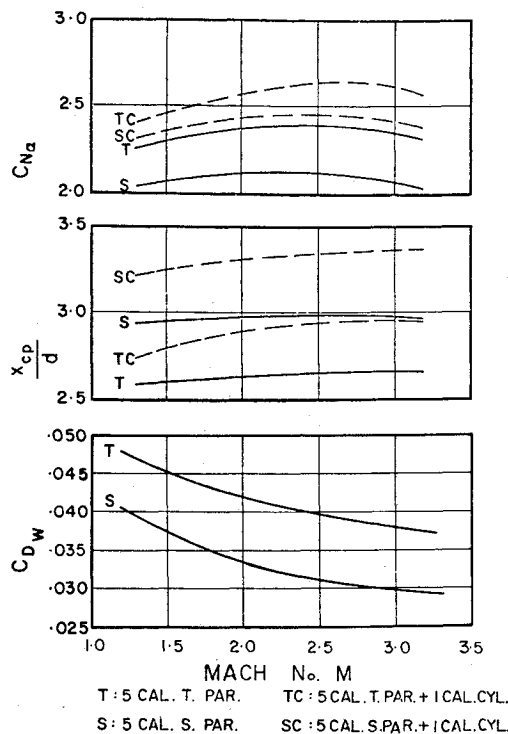


Fig. 6 Comparison of 5-caliber tangent and secant paraboloids with and without a 1-caliber cylindrical afterbody.

Table 2 Comparison of 5-caliber tangent paraboloids (T) and 5-caliber secant (S) paraboloids ( $\delta = 8.5^\circ$ ) with and without a 1-caliber cylindrical afterbody (C)

M		1.5	2.0	3.0
$C_{N\alpha}$	T	2.300	2.373	2.361
	S	2.066	2.102	2.068
	TC	2.452	2.580	2.617
	SC	2.346	2.426	2.408
$X_{cp}/d$	T	2.609	2.654	2.662
	S	2.959	2.973	2.976
	TC	2.783	2.878	2.937
	SC	3.253	3.303	3.327
$C_{Dw}$	T	0.0452	0.418	0.0379
	S	0.0374	0.0333	0.0297

Comparison of volumes

Tangent paraboloid:  $(Vol)_T = 0.53333\pi/4 D^2L$

Secant paraboloid:  $(Vol)_S = 0.42399\pi/4 D^2L \approx 80\% (Vol)_T$

The smaller normal forces of the secant configuration in combination with a more rearward center of pressure reduce the destabilizing moments considerably.

A secant ogive (or paraboloid) has, of course, a smaller volume than a tangent ogive (or paraboloid) of the same fineness ratio. If the same volume is required, either a cylindrical portion must be added or a longer secant ogive (or paraboloid) can be used. As an example, a calculation has been made for a 6-in-diam shell with 3 different forebodies of the same volume, and a 0.453 caliber boattail of  $6^\circ$ . The basic forebody was a 5-caliber tangent paraboloid (conf. 1). This was compared with a forebody consisting of a 5-caliber secant paraboloid ( $8.5^\circ$  semivertex angle) plus a 0.547 caliber cylindrical section (conf. 2), and with a longer secant paraboloid of 6.3 caliber and a  $6.76^\circ$  semivertex angle (conf. 3). Figure 7 and Table 3 show the configurations and the aerodynamic data for  $M=3$ . To have a proper comparison of the gyroscopic

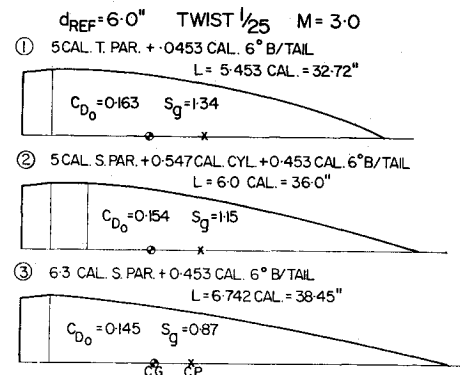


Fig. 7 6 in-diam shell with  $6^\circ$  boattail and various forebodies of same volume.

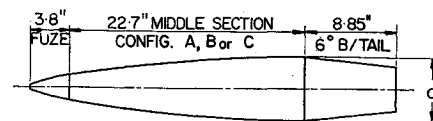
Table 3 6-inch. diam shell with a  $6^\circ$  boattail of 0.453  $d$  length and various forebodies of same volume ( $d = 6$  in.)<sup>a</sup>

Configuration	1	2	3
Total length $L$ , in.	32.718 (5.453 $d$ )	36.0 (6.0 $d$ )	38.452 (6.742 $d$ )
Weight, lb.	69.9	69.9	69.1
c.g., in. from base	11.25	11.79	12.02
$I_{xx}$ , lb-in. <sup>2</sup>	308.9	293.0	279.2
$I_{yy}$ , lb-in. <sup>2</sup>	3891	4591	5262
$C_{N\alpha}$	2.43	2.35	2.18
c.p., in. from base	16.32	16.44	17.28
$C_{D0}$	0.163	0.154	0.145
$S_g$	1.34	1.15	0.87

<sup>a</sup> Note: 155 mm gun with twist of 1:25;  $C_{D0}$  calculated with 5% interference drag.

stability, equivalent internal mass distributions were assumed to give approximately the same weight. The use of the secant forebodies reduces the total drag by more than 5% and 10% for configurations 2 and 3, respectively; however, the gyroscopic stability also decreases such that the long secant forebody becomes unacceptable.

The situation changes if the nose section and afterbody are given and the best midsection contour of constant length and volume is required. An example calculation at  $M=2.0$  for a 6 caliber shell with a fuze as a nose section and three different midsections (Fig. 8) shows that the drag increases from the



3.8" FUZE + 22.7" MIDDLE SECTION + 8.85"  $6^\circ$  B/TAI  
 $d = 5.885$  TOTAL LENGTH  $L = 35.35$

MIDDLE SECTION :- A - PART OF 5 CAL. TANGENT PAR.  
B - 17.5" SECANT PAR. + 5.2" CYL.  
C - 15.5" CONICAL + 7.2" CYL.

THEORETICAL RESULTS FOR  $M=2$

CONFIG.	$C_{D0}$	$C_{N\alpha}$	$X_{cp}$
A	0.194	1.955	27.20
B	0.197	1.989	26.00
C	0.210	2.067	25.80

$X_{cp}$  INCHES FROM BASE

Fig. 8 Comparison of configurations with fuze.

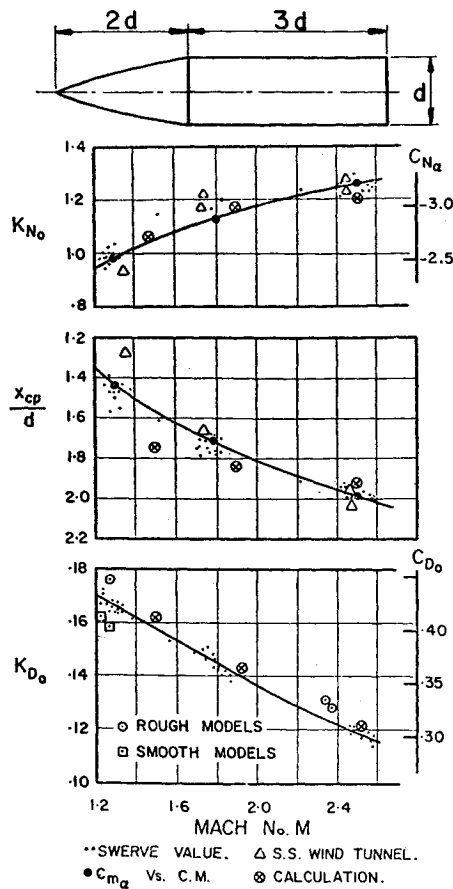


Fig. 9 Tests results of a 5-caliber shell (2-caliber secant ogive + 3-caliber cylinder) and comparison with theory.

tangent to the secant and (the limiting) conical form so that in this case the tangent ogival (or parabolic) contour is the most favorable regarding drag.

Since aerodynamic design charts are not available for secant ogives it is of interest to check the second order shock expansion method in this case. Results of secant ogive-cylinder configurations for Mach numbers between 1.2 and 2.6 are available from test firings of the Ballistic Research Laboratories.<sup>9</sup> The models of 20 mm diam had a 2 caliber secant ogive nose whose radius was twice the tangent ogival radius, and cylindrical afterbodies of 3, 5, and 7 calibers. Because of the small fineness ratio of the forebody and the small Mach numbers they are a good choice for comparison with theory. The theoretical calculations were made for  $M = 1.5, 1.9$ , and  $2.5$ , and the results are shown in Fig. 9 for the configuration with the 3 caliber afterbody as an example. The agreement with the experimental results can be regarded as quite satisfactory even in the low Mach number range.

### Flares (Conical Frustra)

The initial purpose of the present study was to obtain reliable data for conical flares behind a forebody. Information available from handbooks and design charts<sup>1,2</sup> give only results based on the Newtonian impact theory or on data for a cone minus the truncated tip, viz.,

$$C_{N\alpha} = C_{N\alpha \text{ cone}} (D^2/d^2 - 1) \quad (5)$$

$$X_{cp} = L/3 \frac{2D/d + 1}{D/d + 1} \quad (6)$$

$$C_{Dw} = C_{D \text{ cone}} (D^2/d^2 - 1) \quad (7)$$

where  $D$  and  $d$  are the diameters and  $L$  the length of the frustrum. The reference area for the above formulae is  $S_{ref} = (\pi/4) d^2$ .

These data are apparently not correct if applied to a frustrum behind a long cylinder and for low supersonic Mach numbers. It was therefore recommended by Elinwood et al.<sup>10</sup> to reduce the above  $C_{N\alpha}$  by 10%. Tests mentioned in another report<sup>11</sup> showed that a reduction by 20% was more appropriate. The actual reduction however, depends very strongly on length and angle of flare and the Mach number, as calculations with the second-order shock expansion method show. In Fig. 10 the ratio of the actual  $C_{N\alpha}$  to that of the truncated cone value [Eq. (5)] for a Mach number of  $M = 3$  is given. It can be seen that even 80% reductions are possible, e.g., in the case of a  $10^\circ$  flare with a 0.5 caliber length. Similarly the drag and the center of pressure change considerably from those with the above formulas (6) and (7). Figure 11 (taken from Ref. 5) shows this for a 2 caliber  $10^\circ$  frustrum preceded by a semi-infinite cylinder, over the Mach number range from  $M = 2$  to 6.

The method has been applied to a configuration with flares, for which test results over the Mach number range from 1.8 to 4.23 are available.<sup>12</sup> The test configurations, 13.1 caliber long, consist of a 5.1 caliber cone—6 caliber cylinder combination followed by a 2 caliber flare with  $10^\circ$  and  $13^\circ$  flare angle, respectively. Figure 12 compares the test data with the theoretical results. The comparison again confirms the usefulness of the second-order shock expansion method for design studies, whereas the Newtonian theory considerably overestimates the stability, underestimates the drag and therefore may lead to an unsatisfactory design.

In cases where the cylinder preceding the flare is very long as in the aforementioned case, quick estimates can also be obtained by using characteristics of flares preceded by a semi-infinite cylinder; these characteristics can be read off from charts obtained with the second order shock expansion method. The flare data differ only slightly from those obtained with the actual forebody.

### Effect of Forebody on Afterbody

It is evident that the length and the form of the forebody have a significant influence on the afterbody. This is easily seen if the example of a frustrum is taken with a cone as forebody. If the cone vertex angle is the same as that of the

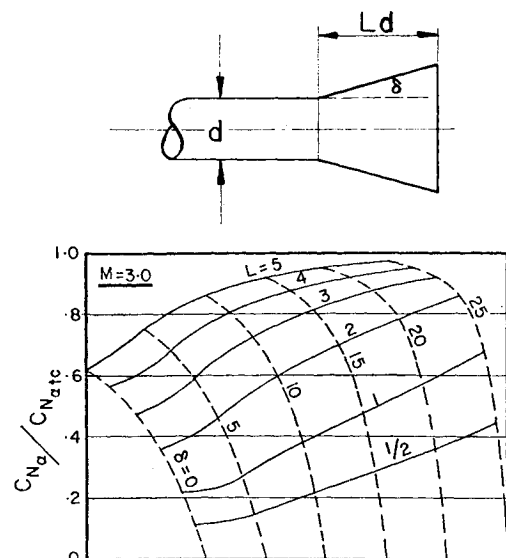


Fig. 10 Effect on the  $C_{N\alpha}$ -ratio by varying the length and angle of a frustrum preceded by a semi-infinite cylinder.

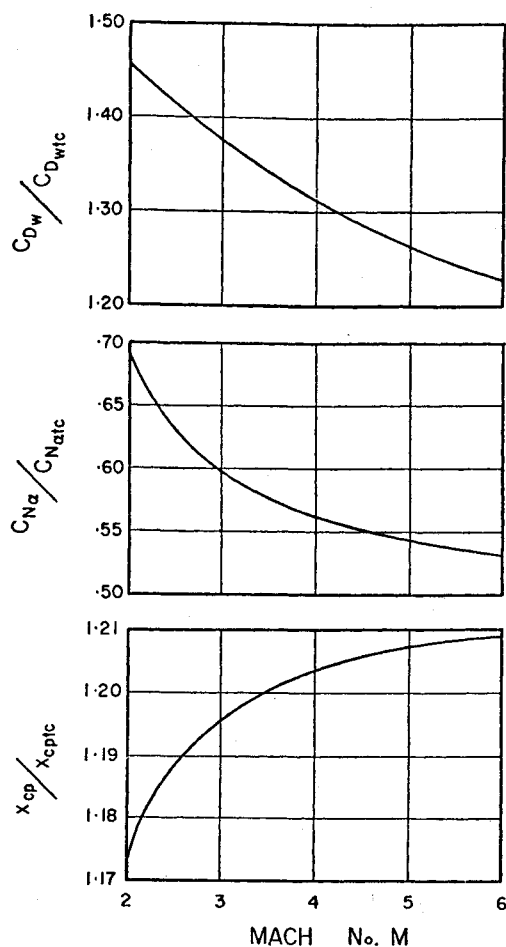


Fig. 11 Mach effect on normal force, drag, and center of pressure ratios for a 2-caliber frustrum of 10° semi-vertex angle preceded by a semi-infinite cylinder.

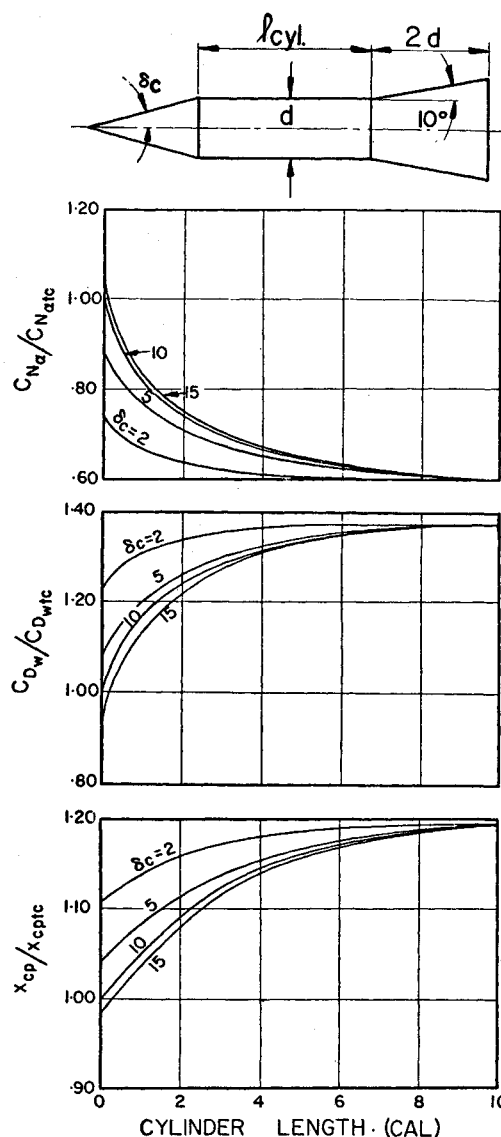


Fig. 13 Forebody effect (cone and midcylinder variations) on the aerodynamic characteristics of a 2-caliber 10° frustrum

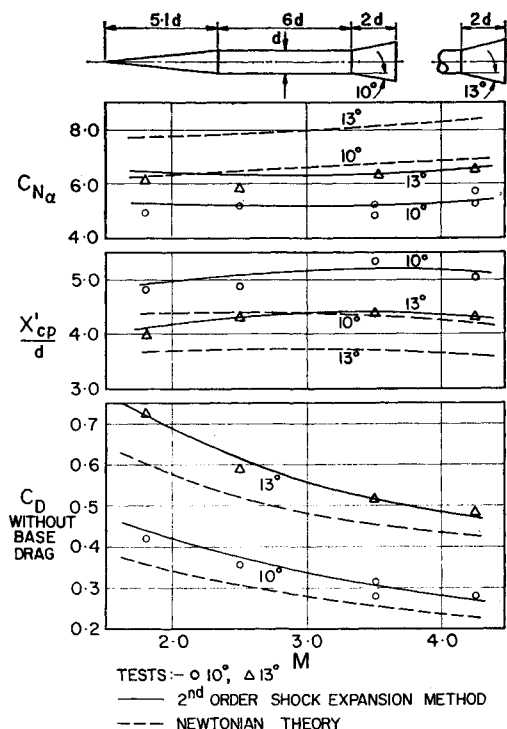


Fig. 12 Test result of cone-cylinder-flare configurations and comparison with theory.

frustrum, a single cone results, and the "frustrum" data are exactly that of Eqs. (5-7). If the cone vertex angle decreases (i.e., the cone length increases) the frustrum's  $C_{Na}$  decreases and the  $C_D$  increases towards the data obtained for a semi-infinite cylindrical forebody. The tendency goes the other way if the cone angle is larger than that of the frustrum. This is well illustrated in Fig. 13 (taken from Ref. 5) which also includes the effect of the length of a cylindrical section between cone and frustrum. As expected, the longer the cylinder, the less the influence of the nose cone angle, and the data converge towards those of a frustrum preceded by a semi-infinite cylinder.

### Conclusion

A few examples show that the second-order shock expansion method, properly applied, gives useful results of a general nature. It is also a valuable tool when comparing various configurations in order to obtain the optimum design. Parabolic and ogival contours give negligible differences in aerodynamic characteristics. Secant ogives are found to have lower drag and more favorable stability coefficients. Applied to flares, the method shows that the aerodynamic characteristics depend strongly on Mach number, flare length and angle, and

differ considerably from the data obtained with the Newtonian impact theory. Furthermore the method allows results for any arbitrary meridian line of the body, in particular the effect of forebody on the afterbody; it is, therefore, useful in cases for which no aerodynamic charts are available. In all cases studied, the agreement of theoretical and experimental results is very good. Using a digital computer program, quick and reliable results are obtained at very low cost. The results for configurations studied in this paper were obtained at an average of approximately 70–80 cents per configuration and Mach number, using an IBM 360–75 digital computer. The method, therefore, fulfills all the requirements for a quick, handy, simple and inexpensive method for preliminary design calculations where more sophisticated theoretical methods and wind tunnel tests or aeroballistic firings would be prohibitive as to cost and time.

### References

- <sup>1</sup> Ellison, D. E., "USAF Stability and Control Datcom," McDonnell Douglas Corp., Douglas Aircraft Div., Oct. 1960, revised June 1969, Flight Control Div., Air Force Flight Dynamics Lab., Wright-Patterson Air Force Base, Ohio.
- <sup>2</sup> "Design of Aerodynamically Stabilized Free Rockets, Engineering Design Handbook," AMCP 706-280, July 1968, H.Q. U.S. Army Materiel Command.
- <sup>3</sup> *Royal Aeronautical Society Data Sheets, Aerodynamics*, London, England, Fourteenth Issue, July 1963.
- <sup>4</sup> Syvertson, C. A. and Dennis, D. H., "A Second Order Shock Expansion Method Applicable to Bodies of Revolution near Zero Lift," Rept. 1328, 1957, NACA.
- <sup>5</sup> Maidment, P. E., "The Static Stability of Bodies of Revolution in Supersonic Flow—Effect of Forebody on Afterbody," Master's thesis, 1972, McGill Univ., Montreal, Canada.
- <sup>6</sup> Ferrari, C. "The Supersonic Flow about a Sharp Nosed Body of Revolution," Translation A9-T-18, 1948, Graduate Div. of Applied Mathematics, Brown Univ., Providence, R. I.
- <sup>7</sup> Mölder, S., "Reflections of Curved Shock Waves," I.C.A.S. Paper 70-11, Sept. 1970; also *C.A.S.I. Transactions*, Vol. 4, No. 2, Sept. 1971, pp. 73–80.
- <sup>8</sup> Geber, N. and Bartos, J. M., "Tables for Determination of Flow Variable Gradients Behind Curved Shock Waves," BRL Rept. 1086, Jan. 1960, Ballistic Research Labs., Aberdeen Proving Ground, Md.
- <sup>9</sup> Murphy, C. H. and Schmidt, L. E., "The Effect of Length on the Aerodynamic Characteristics of Bodies of Revolution in Supersonic Flight," BRL Rept. 876, Aug. 1953, Ballistic Research Labs., Aberdeen Proving Ground, Md.
- <sup>10</sup> Elinwood, J. W., Parsons, W. D., and Nakagama, T. T., "Effectiveness of Flared Afterbodies in Lift: Data Survey and Application to the Exos Third Stage," Space General Rept. 106-R2, May 1962, Space-General Corp. (now Aerojet-General Corp.) El Monte, Calif.
- <sup>11</sup> Mathur, M. C., "The Static Stability of a Cone-Cylinder Flare and Two Cone-Cylinder Fin-Flare Combinations at Supersonic Speed," *The Aeronautical Journal of the Royal Aeronautical Society*, Vol. 73, June 1969, pp. 520–524.
- <sup>12</sup> Ohman, L. H., "A 'Square' Flare—A Second Note," *AIAA Journal*, Vol. 6, No. 12, Dec. 1968, pp. 2449–2450.